Iranian Journal of Analytical Chemistry
Volume 7, Issue 1, March 2020 (57-63)

مجله ایرانی شیمی تجزیه
دوره۷، شماره ۱، فروردین ماه ۱۳۹۹ (۶۳-۵۷)

Synthesis and Application of Magnetic Fe_3O_4-Walnut Sawdust Nanocomposite for Removal of Lead from Water

Fatemeh Sabermahani*, Fariba Honarmand
Department of Chemistry, PayameNoor University, P.O. Box19395-4697, Tehran, IRAN
Received: 18 January 2020 **Accepted:** 24 March 2020
DOI: 10.30473/ijac.2020.51005.1163

Abstract
In this study, Magnetic Fe_3O_4-walnut sawdust nanocomposite was synthesized and used for removal of lead from aqueous solution. The size, structural, optical and morphological properties of nanoparticles have been analyzed by Scanning Electron Microscope (SEM) and Dynamic Light Scattering method. The effect of pH, contact time, adsorbent dose, initial concentration, ionic strength and the effect of temperature on the adsorption was checked out in a batch process mode. Using the equilibrium constants obtained at different temperatures, the thermodynamic results parameters were calculated as ΔG, ΔH and ΔS. The thermodynamic parameters showed that the uptake of lead is spontaneous and endothermic. The data were fitted with the Langmuir and Freundlich equations to describe the adsorption equilibrium. The maximum adsorption capacity by using Langmuir equation was calculated 12.99 mg/g. The kinetic data followed by Pseudo second. Owing to such outstanding features, Magnetic Fe_3O_4-walnut sawdust nanocomposite proved the great potential in adsorption lead removal from aqueous solutions.

Keywords
Removal; Lead; Magnetic Fe_3O_4- Sawdust; Nanocomposite; Kinetics.

1. INTRODUCTION

During the past decades, heavy metals have emerged as a major inorganic pollutant and threat to natural environment and human health. The only solution to protect the environment and human health is their removal from metal laden wastewater before discharging them into aqueous streams. These metal ions, primarily originate from electroplating, mining and ore processing, paint, chemicals and fertilizer industries and metal surface treatment processes [1-3]. Lead is more toxic as compared to other heavy metals like cobalt, manganese, zinc and copper. Exposure to lead may cause abdominal pain, sterility, neonatal deaths, damages the liver and kidney, nervous system, and the process of hemoglobin synthesis, porphyrin metabolism by forming complexes with oxogroups in enzymes [1,2,4]. Therefore, it is essential to remove lead from water before being released into bodies .

Several technologies are in use for lead removal. These technologies include ion exchange, chemical precipitation, electrolysis, membrane separation and adsorption. Amongst these, adsorption is more reliable and promising owing to its efficiency, local availability of adsorbents, operational simplicity, cost effectiveness and regeneration potential of the adsorbents [5-8]. Nanoparticles are a new group of materials that emphasiszed for the environmental treatment due to their unique properties such as large surface area and pore size, small particle size, surface charge, magnetic property, thermal stability, chemical inertness and biocompatibility [9]. In recent years, several studies have reported the removal of lead from water and wastewater using nanosorbents including, cross-linked melamine based polyamine/CNT composites [10], magnetic chitosan/graphene oxide composites [11], SiO2@OPW nanocomposites [12], Nanocomposite of ZnO with Montmorillonite [13], Magnetic cellulose nanocomposite beads entrapping activated bentonite [14], Graphene oxide-hydrated manganese oxide nanocomposites [15], Nitrogen functionalized mesoporous Carbon[16], CNT/silica nanoparticles [17] and silica nanoparticles[18].

All of these studies revealed that novel applications of nanomaterials for the removal of lead from water. However, so far, there are no reports showing whether magnetic Fe3O4-walnut sawdust nanocomposite (MSD) can be used for removal of lead. This work focused on the one step synthesize and application of MSD for removal of lead.

2. EXPERIMENTAL

1.2. Materials and Instruments

$Fe(NO_3)_3.9H_2O$ (99% wt), walnut sawdust (40-mesh), $Pb(NO_3)_2$ (99% wt), NaOH (99.5% wt), Na_2SO_4 (95% wt), $CaCl_2.2H_2O$ (97% wt), Ammonia solution, (all from Merck Co,

*Corresponding Author: fatemehsaber2003@yahoo.com

Germany). Standard solutions of lead ions (1000 ppm) were prepared by dissolving of $Pb(NO_3)_2$ salt in the distilled water.A SensAA GBC (Dandenong, Australia) atomic absorption spectrometer was used for measurement of lead in air-acetylene flame. A mechanical shaker KS 130 basic (Deutschland, Germany) having speed control and timer was used for batch experiments. A Metrohm pH meter (Herisau, Switzerland) was employed for pH measurements. The concentrations of the lead solutions were obtained using data from a standard calibration curve.

2.2. Preparation of magnetic sawdust (MSD)

Walnut sawdust sample was supplied from the local market in Kerman and were ground with a household blender until very smooth fine powder was obtained. The particles were passed through a 40-mesh sieve (with 250 µm in pore size), washed with distilled water and dried in 25 °C. Magnetic sawdust was prepared through a simple and one-step method in which preparation Fe_3O_4 and bonding to the sawdust was performed simultaneously. In a typical reaction procedure, 4.0 g sawdust as a reducing agent was added to 50 ml water containing $Fe_3O_4.9H_2O$ (0.1M). Then, mixture is stirred vigorously for 30 min at 80 °C for reduction of Fe^{3+} ions to Fe^{2+} ions. Then the pH value of the solution was adjusted to around 10.5 by gradually addition of ammonia solution. With continuing vigorous stirring on the heater stirrer, the color of the suspension turned into black immediately. The suspension was cooled to room temperature, and MSD was separated from the suspension with magnetic field and washed several times with distilled water. The obtained magnetic particles were dried at 60 °C and stored for subsequent modification. The proposed reduction mechanism for synthesis Fe_3O_4 is summarized in Fig.1.

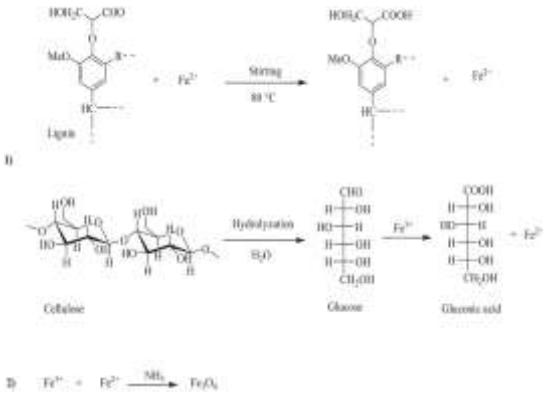

Fig. 1. Proposed reduction for synthesis of Fe_3O_4/SD.

3.2. Characterization of magnetic sawdust (MSD)

The microstructure of magnetic sawdust nanocomposite was observed by Scanning Electron Microscopy (SEM) (Cam Scan MV2300) and is shown in Figure 2. Scanning electron micrographs were recorded without sample coating with 1000x magnification. SEM image of Fe_3O_4/SD showed that Fe_3O_4 nanoparticles incorporate on the surface of sawdust as agglomerated form and other places also. These Fe_3O_4 nps are spherical in shape and prepared using sawdust powder as reducing agent.

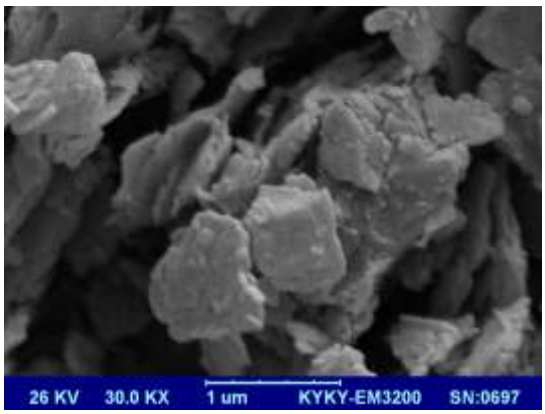

Fig. 2. SEM image of magnetic sawdust.

The Dynamic Light Scattering (DLS) test was also employed to specify the average particle size where its results are available in Figure 3. Accordingly, the average particles size after incorporating of the sawdust was greater than 100 nm.

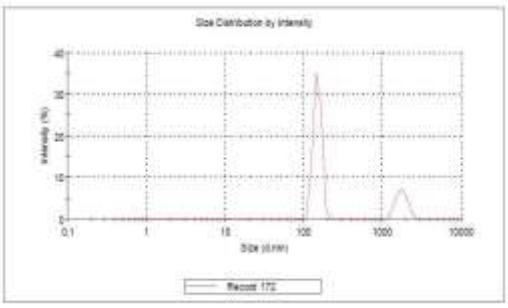

Fig. 3. DLS spectrum of magnetic sawdust (MSD).

4.2. Adsorption method

Batch adsorption experiments were carried out by shaking 0.15 g of the adsorbent (MSD) with 20 ml of the aqueous solutions 30 ppm of lead in stoppered pyrex glass flask, at a fixed temperature. The initial pH of the solutions was adjusted with diluted HNO_3 or NaOH 0.1 M solution and the shaking speed was 200 rpm for 45 min. At the end of the adsorption period, the sorbent was separated from the suspension with magnetic field out and the lead concentration was determined using FAAS.

The amount of Pb(II) ions adsorbed and percentage of removal of Pb(II) ions (Re%) was calculated using Equations (1) and (2).

$q_e = V(C_0 - C_e)/M$ (1)

$Re\% = [(C_0 - Ce)/C_0] \times 100$ (2)

As q_e is the amount of adsorbed Pb(II) ion per gram of the adsorbent, C_0 is initial concentration and C_e is the equilibrium concentration of the Pb(II) (mg L^{-1}) that is obtained from calibration curve and M is the mass of nanocomposite (g).

3. RESULTS AND DISCUSSION

1.3. Effect of pH

The affinity of adsorbent functional sites for lead ions depends on the initial pH of the solution. Lead occurs as Pb^{2+}, $Pb(OH)^{+}$ and $Pb(OH)_2$ species in deionized water. Typically, Pb^{2+} ions exist in the 6.5 pH solution, afterward, in the pH range from 6.5 to 9.0 exist as $Pb(OH)^{+}$. The effect of pH on adsorption of Pb(II) ions was studied over a pH range of 2-8 (Figure 4). The adsorption capacity for Pb^{2+} ions increased from pH 2 to about 6.5. In acidic range functional groups on the sorbent protonated and caused electrostatic repulsion to Pb^{2+} ions. In the alkaline range electrostatic attractions occur between cationic Pb^{2+} ions and anionic adsorbent surface. Further the adsorption of Pb^{2+} reduced above pH 6. Since at pH>6, Precipitation occurs due to forming lead hydroxide, the experiments were performed at pH 6.

The Similar results have been reported for the adsorption of Pb^{2+} ions by other authors [2,6].

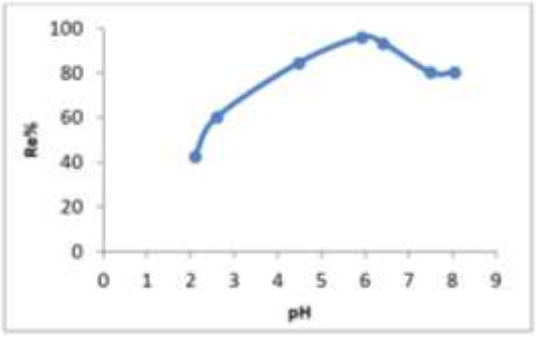

Fig. 4. Effect of pH on the removal of lead.

2.3. Effect of sorbent dose

Effect of adsorbent dosage (m) on the uptake of lead was studied and is shown in Fig. 5. The percent removal of lead increased from 60.4% to 95.9% with an increase in adsorbent amount. The removal of lead at m> 0.15 g remains almost constant. An increase in the removal with the adsorbent dosage can be attributed to greater surface area and the availability of more adsorption sites. At m< 0.15 g, the adsorbent surface becomes saturated with lead and the residual concentration in the solution is large. Thus, the dose of the adsorbent was fixed to 0.15 g for the subsequent adsorption experiment.

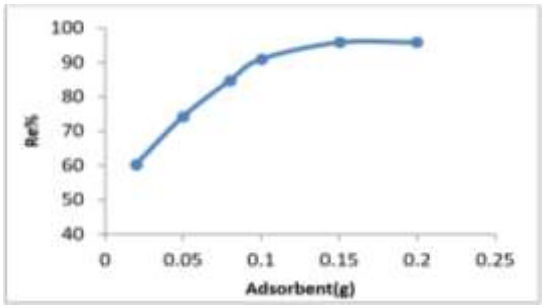

Fig. 5. Effect of adsorbent dosage on the removal of lead on MSD.

3.3. Effect of contact time and initial concentration on Pb(II) *adsorption*

The effect of contact time and Pb(II) concentration is depicted in Fig. 6, 7. The experiments were performed by varying contact time (3–60 min.) and initial Pb(II) concentration (30–150 mg/L) keeping all other parameters constant. The percent removal increased from 65.0% to 95.9% onto composite with time. Pb(II) removal increased continuously upto 45 min and then removal efficiency remains constant. This may be attributed that initially, the active sites for Pb(II) ions are available in excess, but after time equilibrium attained due to the saturation of the sorbent active sites. 45 min was selected for more experiments. Herein the adsorption capacity of the sorbent increased from 3.8 to 12.8 mg/g as the initial concentration of Pb(II) ions increased from 30 to 150 mg/L. These results suggested that the actual amount of Pb(II) ions adsorbed per unit mass of the sorbent increased with Pb(II) ion concentration.

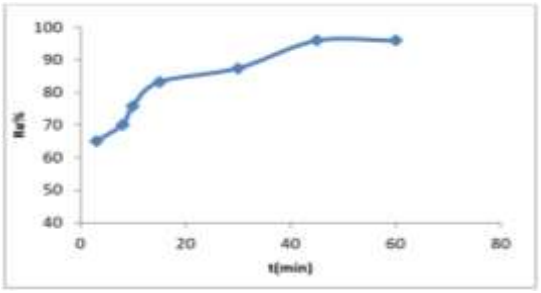

Fig. 6. Effect of contact time on lead adsorption.

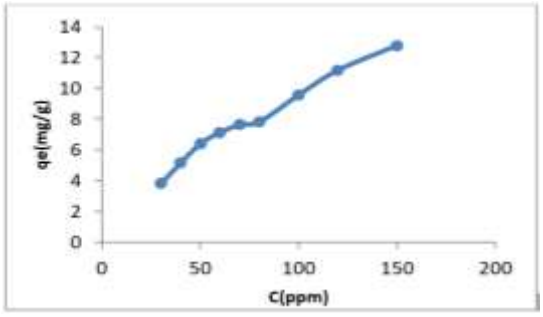

Fig. 7. Effect of initial concentration on lead adsorption.

4.3. Effect of temperature on lead adsorption

The effect of temperature on the adsorption of lead was studied by varying temperature in the range of 14–48°C. The lead removal increased with increase in temperature illustrating that adsorption of lead on the sorbent is endothermic. The Gibbs free energy change, ΔG^0, is fundamental criterion of spontaneity. The sorption process of lead can be summarized by the following reversible process. The equilibrium constant (K_c) is defined as:

$$K_c=(C_0- C_e)/C_e \quad (3)$$

where C_e is the concentration of lead at equilibrium. The K_c value is used in the following equation to determine the ΔG^0 of sorption.

$$\Delta G^0= -RTlnK_c \quad (4)$$

The enthalpy (ΔH^0) and entropy (ΔS^0) can be calculated from the slope and intercept of Vant Hoff equation of ΔG^0 versus T.

$$\Delta G^0= \Delta H^0-T\ \Delta S^0 \quad (5)$$

R the gas constant (8.314 J $mol^{-1}K^{-1}$) and T is the absolute temperature (K). The obtained ΔG^0 values and the adsorption thermodynamic parameters are given in Table 1. The positive value ΔS^0 shows the increase in degree of freedom or increase the disorder of adsorption lead on the sorbent and the positive value ΔH^0 indicates that adsorption process is endothermic.

Table 1. Thermodynamic Parameters for adsorption of lead.

T (K)	ΔG^0 (J mol^{-1})	ΔS^0 (J mol^{-1} K^{-1})	ΔH^0 (kJ mol^{-1})
287	-1273.0	30.92	75.83
290	-1370.3		
305	-1920.8		
310	-2000.4		
315	-2131.4		
321	-2325.8		

5.3. Equilibrium isotherms

To better analyze the equilibrium relationship between lead and the nanocomposite the equilibrium data was examined by two common models: the Langmuir isotherm and the Freundlich isotherm. In this work, both isotherms were used to describe adsorption phenomena on the sorbent. Linear forms of Langmuir and Freundlich isotherm are given in Eqs. (6) and (7).

$$C_e/q_e = (1/Qb) + (1/Q)\ C_e \quad (6)$$

$$Log\ q_e = log\ K_f + 1/n\ log\ C_e \quad (7)$$

q_e is the amount of adsorbed ion per gram of the adsorbent, b is Langmuir constant and *Q* is adsorption capacity expressed in mg g^{-1}, n is the Freundlich constant, and K_f is the adsorption coefficient.

The results showed the Langmuir model yields somewhat better fit for adsorption of lead. All the calculated parameters from intercepted and slope of plots according to Eqs. (6) and (7) are listed in Table 2.

Table 2. Langmuir and freundlich isotherm constants for lead.

T(K)	Langmuir isotherm			Freundlich isotherm		
	Q (mg g^{-1})	B (L mg^{-1})	R^2	K_f	1/n	R^2
298	12.99	0.16	0.94	4.52	0.23	0.87

6.3. Effect of ionic strength

The effect of various amounts of NaCl, $CaCl_2$ and Na_2SO_4 on the sorption of lead on the MSD was examined. It was seen that the there was no significant decrease in the percent removal efficiency. As, even at high concentration of the salt, the MSD still has big percent removal efficiency and can be used to efficiency remove lead from aqueous solutions.

7.3. Adsorption kinetics

The adsorption kinetics described by the relationship between lead uptake and contact time that is discussed by Pseudo-First order and Pseudo-Second order, Eqs. (8,9).

The Pseudo- First order equation is:

$$\log(q_e-q_t) = \log q_e – (k_1/ 2.303)\ t \quad (8)$$

And the Pseudo-Second order equation is:

$$(t/q_t) = (1/k_2\ .\ q_e^2) + t\ /q_e \quad (9)$$

where q_t is the amount of lead adsorbed at 't' time (mg/g), t is the contact time (min), q_e is the amount of lead adsorbed at equilibrium (mg/g), k_1 is the rate constant of Pseudo-First order reaction (min^{-1}) and k_2 is the rate constant of Pseudo-Second-order reaction (g mg^{-1} min^{-1}). The slope and intercept of plot of log (q_e-q_t) against time (min) were used to determine the First order rate constant k_1. The calculated parameters of R^2, $q_{e,cal}$ and $q_{e,exp}$ were listed in Table 3.

Table 3. Adsorption kinetic constants for adsorption of lead on the MSD.

First-order kinetic model				Second-order kinetic model		
q_{exp} (mg.g^{-1})	q_{cal} (mg.g^{-1})	K_1 (L.min^{-1})	R^2	q_{cal} (mg.g^{-1})	K_2 (L.min^{-1})	R^2
3.95	3.05	0.13	0.88	4.01	11.04	0.9978

It was observed that correlation coefficient (R^2) was low and experimental data are not fitted well for Pseudo-First order reaction. Hence, the adsorption mechanism cannot be well described by Pseudo-First order kinetics. The Pseudo-Second order rate constant k_2 was calculated from the slope and intercept of the plot t/q_t against time (Fig. 8). The calculated q_e ($q_{e,cal}$) was in good agreement with experimental q_e ($q_{e,exp}$) with correlation coefficient high (Table 3). These results confirm the well fitting of Pseudo-Second order model for adsorption of lead on to the sorbent.

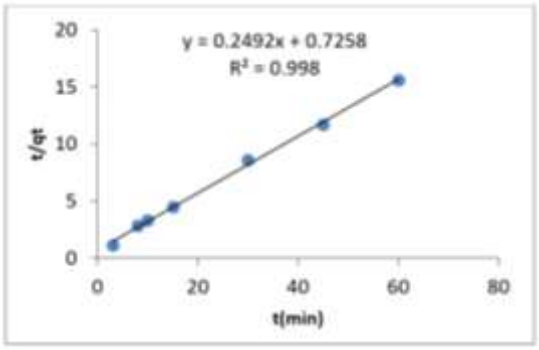

Fig. 8. Pseudo-Second order plot for lead adsorption.

8.3. Desorption

Adsorbed Pb^{2+} ions were removed from the new sorbent using H_2SO_4, HNO_3, H_3PO_4 and HCl with concentrations of 0.1 and 0.5 M. As can be seen from Fig. 9, desorption of lead with H_3PO_4 0.1 M showed the highest desorption percent. However, the results show that the lead adsorbed can be easily desorbed from the sorbent even with low concentration of eluent.

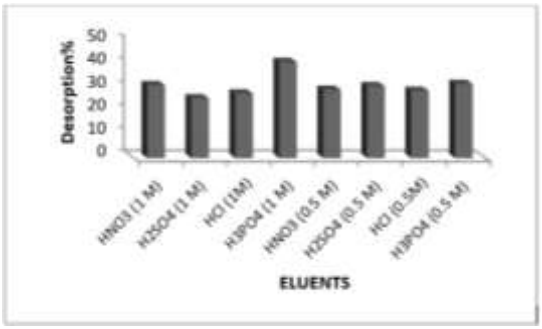

Fig. 9. Comparison of different eluents for recovery of lead.

4. CONCLUSION

In the present paper, a novel adsorbent, magnetic Fe_3O_4-walnut/sawdust (MSD) nanocomposite was synthesized, characterized and applied for removal of lead from water. The dispersion of Fe_3O_4 onto the surface of SD is confirmed by SEM. The optimum adsorbent dosage was 0.15 g at pH=6. The experimental data showed good fit to the Langmuir isotherm. Pseudo-Second order model is best fitted to lead adsorption.

Acknowledgments

The authors would like to express their appreciations to Payame Noor University of Kerman for providing research facilities. This research was supported by the Research Laboratory of Payame Noor University of Kerman.

REFERENCES

[1] O. Charles, A. Hamouz, M.K. Estatie, M.A. Morsy and T.A. Saleh, Lead ion removal by novel highly cross-linked Mannich based polymers, *J. Taiwan Inst. Chem. Eng*. 70 (2017) 345–351.

[2] N.A. Miranda, S. Baltazar, A. Garcıa, D. Munoz-Lira, P. Sepulveda, M.A. Rubioa and D.A.F. Nicolas, Nanoscale zero valent supported by Zeolite and Montmorillonite: template effect of the removal of lead ion from an aqueous solution, *J. Hazard. Mater*. 301 (2016) 371–380.

[3] O.S. Lawal, O.S. Ayanda, O.O. Rabiu, and K.O. Adebowal, Application of black walnut (Juglan) husk for the removal of ion from aqueous solution, *Water Sci. Technol*. 75 (2017) 2454–2464.

[4] M.S. Rajput, A.K. Sharma, S. Sharma and S. Verma, Removal of Lead (II) from aqueous solutions by orange peel, *Int. J. Appl. Res*. 9 (2015) 411–413.

[5] L.F. Musico, C.M. Santos, M.L.P. Dalida, and D.F.R. odrigues, Improved removal of lead(II) from water using a polymer-based graphene oxide nanocomposite, *J. Mater. Chem.* (2013) 3789–3796.

[6] S. Kumar, R.R. Nair, P.B. Pillai, S.N. Gupta, M.A.R. Iyengar, and A.K. Sood, Graphene oxide MnFe2O4 magnetic nanohy-brids for efficient removal of lead and arsenic from, *water. Appl. Mater. Interf*. 6 (2014) 7426-17436.

[7] S. Joshi, V.K. Garg, J. Saini, and K. Kadirvelu, Removal of toulidine blue O dye from aqueous solution by silica-iron oxide nanoparticles, *Mater. Focus*. 7 (2018) 140–146.

[8] P.V. Thitame and S.R.Shukla, Removal of lead (II) from synthetic solution and industry

wastewater using almond shell activated carbon, Environ. Prog. Sustain Energy 36 (2017) 1628–1633.

[9] Y.M. Ahmed, A. Al-Mamun, A. Khatib, M.R., Al, A.T.Jameel and M. AlSaadi, Efficient lead sorption from wastewater by carbon nanofibers, *Environ. Chem. Lett*. 13 (2015) 341–346.

[10] .C.S.A. Hamouz, I.O. Adelabu and T.A. Saleh, Novel cross- linked melamine based polyamine/CNT composites for lead ions removal, *J. Environ. Manage*. 192 (2017) 163–173.

[11] L. Fan, C. Luo, M. Sun, X. Li and H. Qiu, Highly selective adsorption of lead ions by water-dispersible magnetic chitosan/ graphene oxide composites, *Colloids Surf. B* 103 (2013) 523–529.

[12] J. Saini, V.K. Garg and R.K. Gupta, Green synthesized SiO2@OPW nanocomposites for enhanced Lead (II) removal from water, *Arabian J. Chemistr*, In Press.

[13] H.A. Sani, M.B. Ahmad, M.Z. Hussein, N.A. Brahim and T.A. Saleh, Nanocomposite of ZnO with montmorillonite for removal of lead and copper ions from aqueous solutions, *Process Saf. Environ. Protect*. 109 (2017) 97–105.

[14] X. Luo, X. Lei, X. Xie, B. Yu, N. Cai and F. Yu, Adsorptive removal of Lead from water by the effective and reusable magnetic cellulose nanocomposite beads entrapping activated bentonite, *Carbohyd. Polym*. 151(2016) 640–648.

[15] S.Wan, F. He, J. Wu, W. Wan, Y. Gu and B. Gao, Rapid and highly selective removal of lead from water using graphene oxide-hydrated manganese oxide nanocomposites, *J. Hazard. Mater*. 314 (2016) 32–40.

[16] G.Yang, L. Tang, G. Zeng, Y. Cai, J. Tang, Y. Pang and Y. Zhou, Simultaneous removal of lead and phenol contamination from water by nitrogen-functionalized magnetic ordered meso- porous carbon. *Chem. Eng. J*. 259 (2015) 854–864.

[17] T.A. Saleh, Nanocomposite of carbon nanotubes/silica nanoparticles and their use for adsorption of Pb (II): from surface properties to sorption mechanism, *Desalination Water Treat*. 57 (2016) 10730-10744.

[18] J. Liu, X. Yang, Z. Shen, B. Zhang, J. Yang, W. Hong and Z. Zhuang, Silica nanoparticles capture atmospheric lead: Implications in the treatment of environmental heavy metal pollution, *Chemosphere* 90 (2013) 653-656.

سنتز و کاربرد نانوکامپوزیت مغناطیسی خاک اره/Fe_3O_4 برای حذف سرب از آب

فاطمه صابرماهانی*، فریبا هنرمند

بخش شیمی، دانشکده علوم، دانشگاه پیام نور، تهران، ایران

تاریخ دریافت: ۲۸ دی ۱۳۹۸ تاریخ پذیرش: ۵ فروردین ۱۳۹۹

چکیده

در این کار نانو کامپوزیت خاک اره/نانوذره مغناطیسی سنتز و برای حذف سرب از محیطهای آبی استفاده گردید. سایز، ساختمان، خواص مورفولوژی و ریخت-شناسی با دستگاه‌های میکروسکوپ الکترونی روبشی SEM و روش پراکندگی نوری DLS مورد آنالیز و بررسی قرار گرفت. pH، زمان تماس، مقدار جاذب، غلظت کاتیون، قدرت یونی و اثر دما و با استفاده از روش ناپیوسته مطالعه شد. با استفاده از ثابت‌های تعادلی بدست آمده در دماهای مختلف، پارامترهای ترمودینامیکی مثل $⟦\Delta H⟧^0$,$⟦\Delta S⟧^0$,$⟦\Delta G⟧^0$ محاسبه شدند. پارامترهای ترمودینامیکی در این آزمایش نشان داد که فرآیند جذب سرب خودبخودی و گرماگیر است. ایزوترم‌های جذب سطحی لانگمویر و فروندلیچ برای توصیف تعادل جذب استفاده شد. مشخص گردید داده‌های مربوطه تطابق بهتری با مدل فروندلیچ دارند. حداکثر ظرفیت جذب با استفاده ازمعادله لانگمویر ۱۲,۹۹ میلی‌گرم بر گرم محاسبه شد. داده‌های سینتیکی با شبه مرتبه دوم مطابقت داشتند. مطالعه به این نتیجه رسید که خاک اره/ نانوذره مغناطیسی می‌تواند پتانسیل خوبی برای حذف یون‌های سرب از محیطهای آبی داشته باشد.

واژه‌های کلیدی

حذف؛ سرب؛ خاک اره–نانوذره مغناطیسی؛ نانوکامپوزیت؛ سینتیک.